PAMAP

Deliverable: D6.3

Issue 0.1

System Evaluation Report

		Name (company)	Date
Approved	Task T6.3 Leader	Laetitia Fradet (UTC)	**31 January 2011**
	Hierarchical responsible	Frédéric Marin (UTC)	**31 January 2011**
Verified	WP6 Leader	Gabriele Bleser (DFKI)	**31 January 2011**
Released	Coordinator	Didier Stricker (DFKI)	**31 January 2011**

Dissemination level: PU
PU *(Public);* ***PP*** *(Restricted to other programme participants);* ***RE*** *(restricted to a group specified by the consortium);* ***CO*** *(confidential only for members the consortium)*
Document Status: *final*

COVER AND CONTROL PAGE OF THE DOCUMENT	
Project EU reference:	AAL-2008-1-162
Project acronym:	PAMAP
Project Title:	Physical Activity Monitoring for Ageing People
Work package	WP6: System Integration and Trials
Task	T 6.4: System evaluation
Deliverable number:	D6.3
Document title:	System Evaluation Report
Document type (PU, INT, RE)	PU
Version:	1.0
Date:	31/01/2011
Author(s):	Laetitia Fradet (UTC),
Contributors list:	Nathalie Ville (CIT-Rennes), Lamprinos Ilias (ICOM), Attila Reiss (DFKI), Gabriele Bleser (DFKI), Oliver Machui (Trivisio)

Table of Contents

Table of Figures

Table of Tables

EXECUTIVE SUMMARY

PAMAP project aims at developing a system that enables the accurate monitoring of the physical activities of aging people. This deliverable provides the reader with all activities related to the first evaluation of the system under development.

In Chapter 1, the evaluation will address the technical evaluation of the system components. More specifically, Chapter 1.1 will tackle the CE-Compliance of sensors. Chapter 1.2 will develop on the estimation of the accuracy of body tracking whereas the chapter 1.3 will develop the performance of activity classification and activity intensity estimation. Chapter 1.4 will evaluate the sensor fastening.

In Chapter 2, the evaluation will address the software parts of the PAMAP system, i.e. the infrastructure and a set of applications that facilitate out-of-hospital physical activity monitoring for prevention and rehabilitation.

This document will serve as a basis for the User Requirements Task and the corresponding deliverables that are also part of Work Package 2: PAMAP System Requirements and Design.

1.1 CE-Compliance of sensors

The CE compliance of the cable based inertial motion sensor "Colibri" contains three aspects: product safety, EMC (electromagnetic compatibility) and documentation. Trivisio performed several tests, some of them in special laboratories, to check these aspects.

1.1.1 Product Safety

The device is using low voltage, only 5V, and the case is from aluminum and waterproof. This means that the sensor can be used without risk even in wet conditions and i.e. sweating. The sensors can be used safely, if usage is in normal conditions and if the user is paying attention to the cable not being entangled around his neck.

The device was tested in rough environments, wide temperate ranges (-10°-40°C), shocks, high pressure and under water (30m). The underwater tests have been performed in a special laboratory with a pressure chamber.

1.1.2 Electro Magnetic Compatibility

These tests were conducted in a special EMC laboratory. Trivisio defined the standard to be conform to: DIN EN 61326-1 (Electrical equipment for measurement, control and laboratory use). The following tests have been performed:

1) Emission

First, the emission was measured. The sensor showed nearly no radiation, all signals were below the limits (red line in diagram below).

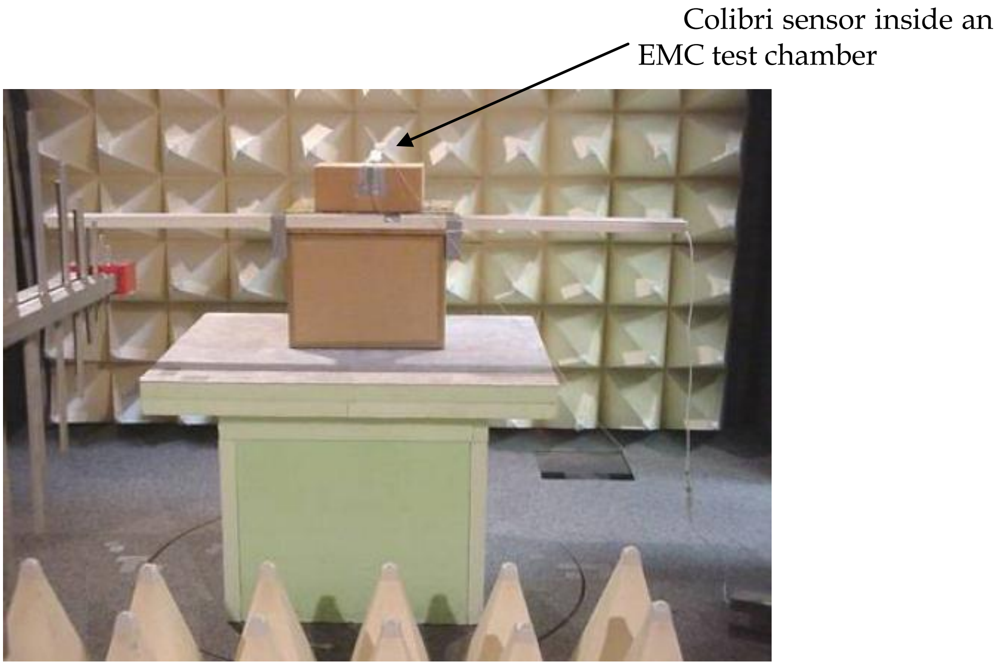

Figure 1: Colibri sensor inside an EMC test chamber

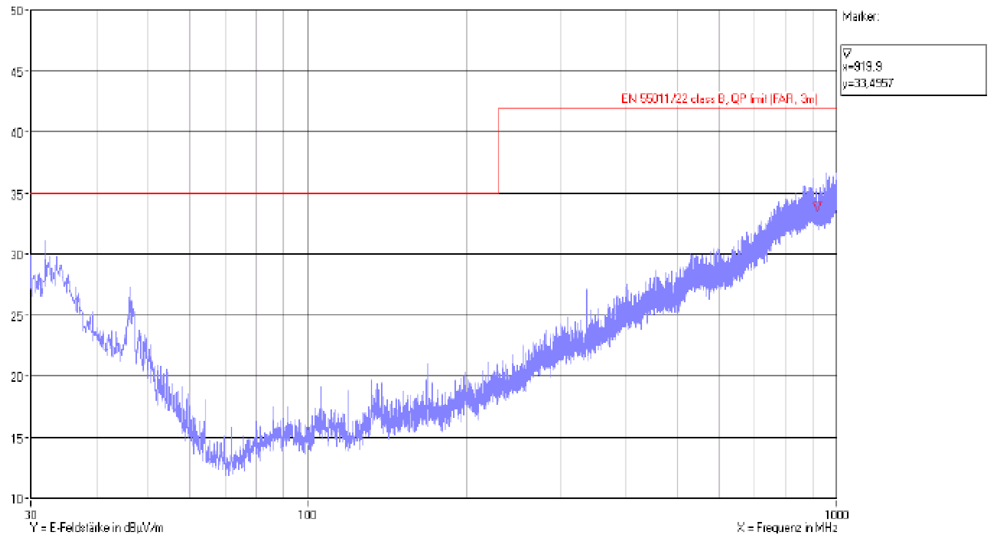

Graph 1: Radiated emissions, horizontal, front side

Figure 2: Colibri sensor emission diagram

2) RF Immunity

During this test conducted RF (radio frequency) in the range of 150 kHz-80MHz was tested in the cable and case. The sensor stopped working but had no damage and continued working after restart. This is in accordance with the norm.

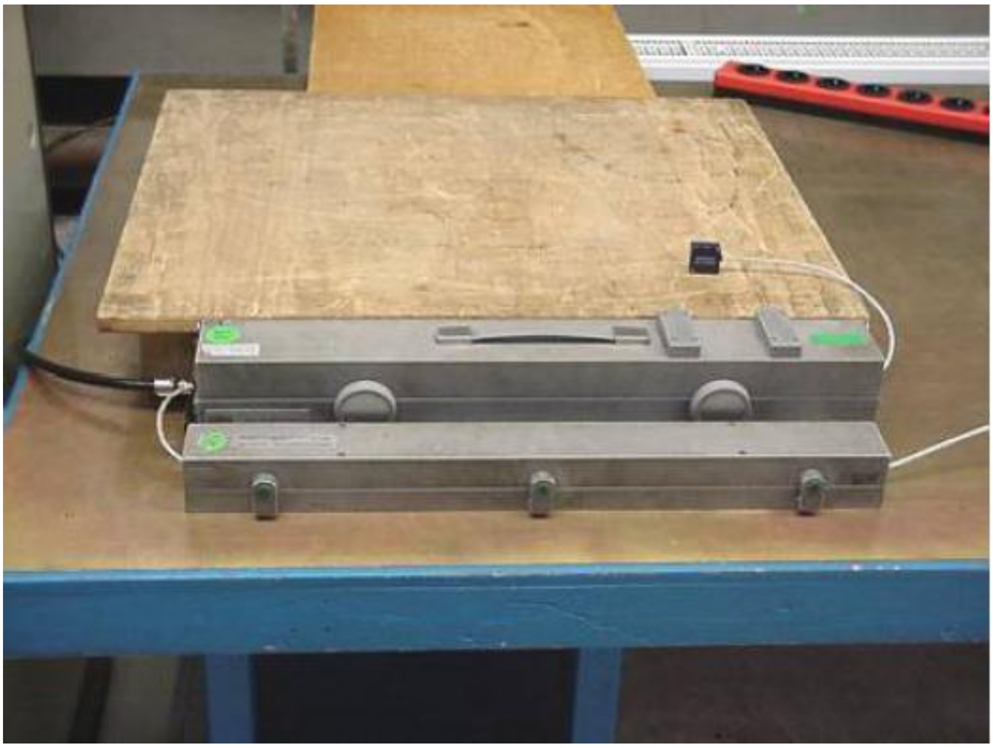

Figure 3: Colibri sensor with conducted RF on cable

3) Electrostatic discharge (ESD) immunity

A contact discharge of about ± 4kV to the aluminum case of the sensor was applied with a special high voltage pistol. In a first attempt the sensor failed this test. It stopped working (but resumed after reboot). This is not acceptable according to the selected norm. After minor modifications of the shielding and better ground connection to the cable the test was passed successfully.

Figure 4: Colibri sensor in ESD test

4) Power frequency magnetic field immunity

For this test the sensor was placed in the center of a Helmholtz coil and a magnetic field was applied. The sensor also passed this test and measured the magnetic field with its integrated magnetometers in all 3 axes.

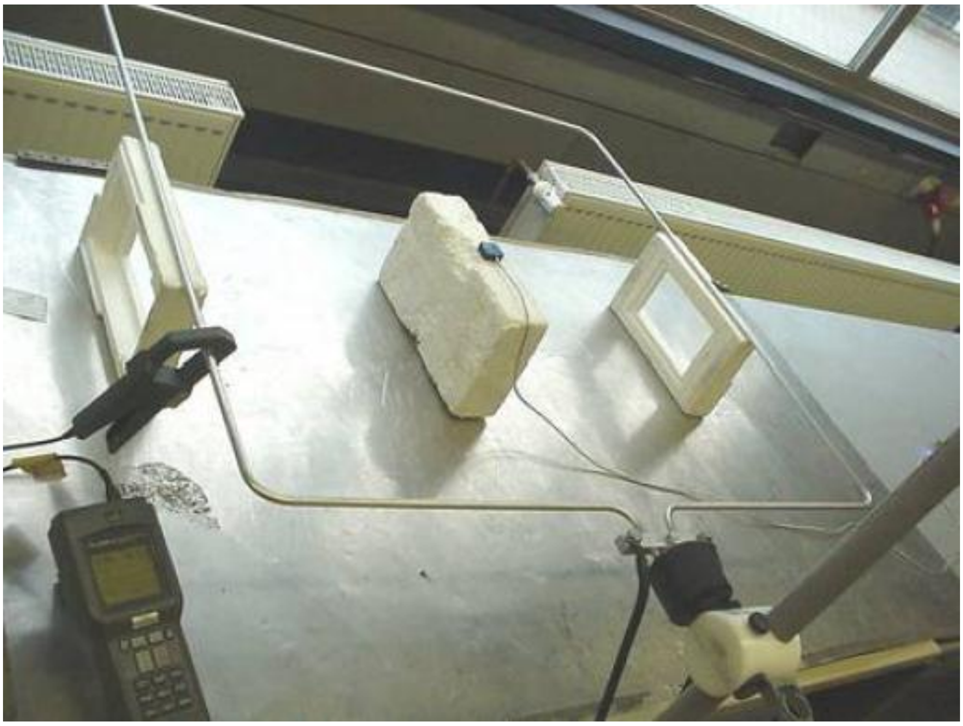

Figure 5: Colibri inside the power frequency magnetic field

1.1.3 Documentation

This part concerns the availability of a user manual and documentation of the manufacturing details. The manual is available on Trivisio's website for download and as part of the software installation.

1.1.4 Results

Trivisio successfully certified EMC tests with the Colibri sensor according to DIN EN 61326-1 norm. Newly manufactured cases can be labeled with the CE sign.

1.2 Accuracy of body tracking

This part of the evaluation aims at evaluating the measurement system and the biomechanical model used. Both of them are indeed potential sources of errors in measures.

The protocol followed confronts the results obtained thanks to the PAMAP system with those obtained through validated method/system. Since the PAMAP system is devoted to body tracking and as such incorporates hypotheses on body joints, the system could not be evaluated by tracking a frame which size and movement would have been known but it was evaluated when tracking human body.

The present evaluation focused on upper-extremities since the biomechanical model proposed is original and has not been yet validated.

1.2.1 Methodology

A validated optoelectronical motion capture system (Vicon, Oxford Metrics) was used in parallel with the PAMAP body tracking system. Reflective markers were placed at anatomical landmarks following a validated upper-extremity model (Rettig et al. 2009). Reflective markers were also placed on the IMUs of the PAMAP body tracking system as depicted on Figure 1. This was done in order to enable the tracking of the position of the IMUs with the validated motion capture system.

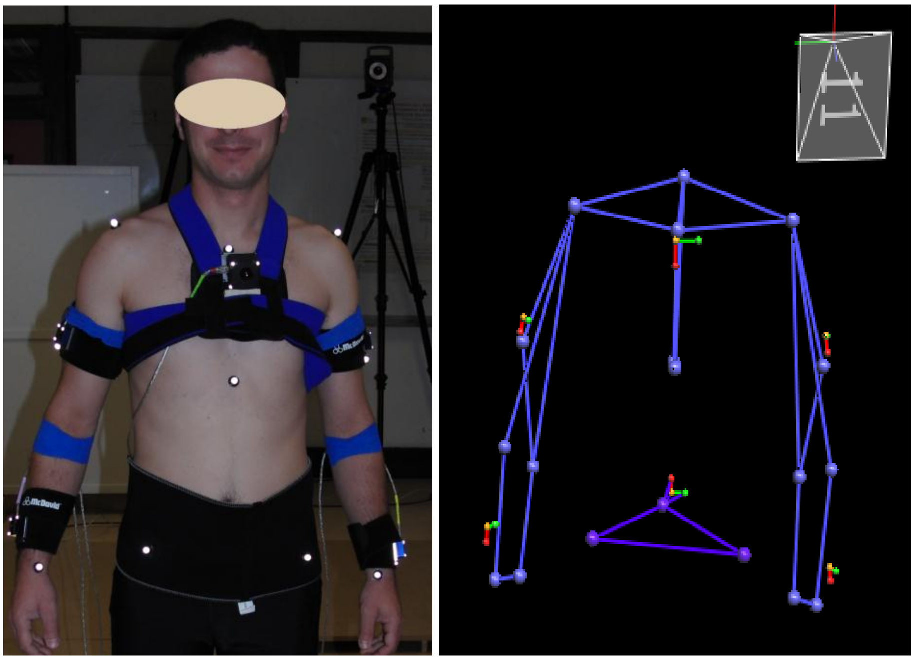

Figure 6: Markers' placement

Three different subjects were measured. They first performed the required movements for the biomechanical model calibration (both for the validated model and for the model used by the PAMAP system) and then some typical rehabilitation movements such as biceps curls or pushups so that all the upper-extremity joints were used.

The Euler angles measured at each joint were then computed by three different means:

- by using the reflective markers placed on anatomical landmarks and the biomechanical model proposed by Rettig et al. (2009). This provides a measure of the body segment rotation thanks to a validated motion capture and a validated biomechanical model. These data will be later referenced as Mref.
- by using the reflective markers placed on the IMUs and the biomechanical model proposed within the current project (see deliverable D4.2). This provides a measure of the body segment rotation thanks to a validated motion capture and the biomechanical model to evaluate. These data will be later referenced as Mmodel.
- by using the IMUS data and the model proposed within the current project. This provides a measure of the body segment rotation thanks to the motion capture and the biomechanical model to evaluate. These data will be later referenced as Mimu.

The formalism proposed to express the Euler angles was the one recommended by the International Society of Biomechanics (Wu et al. 2005). The body axes were defined as depicted on Figure 2. This formalism was chosen in order to be consistent with traditional biomechanical publications but also to be able to better interpret the results in terms of anatomy.

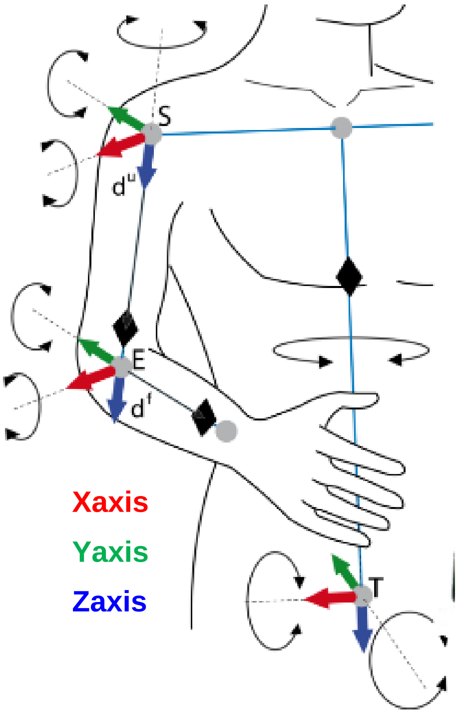

Figure 7: Definition of the body axes.

The comparison of the data between Mref and Mmodel provides an evaluation of the biomechanical model alone whereas the comparison between Mmodel and Mimu provides an evaluation of the measurement system.

Three different parameters were computed to compare the results. The first one was the difference of the mean Euler angle obtained during the movement performed. This parameter provided an estimation of the offset existing between the data. The second parameter was the difference of the Euler angle range of motion obtained during the movement performed. It gives insight on the resolution differences between the data but also on difference on the body axes. The last parameter was the coefficient of correlation between the Euler angles obtained through the different methods, which provides an estimation of the synchronicity of the measurements.

1.2.2 Validation of the biomechanical model: Mref vs Mmodel

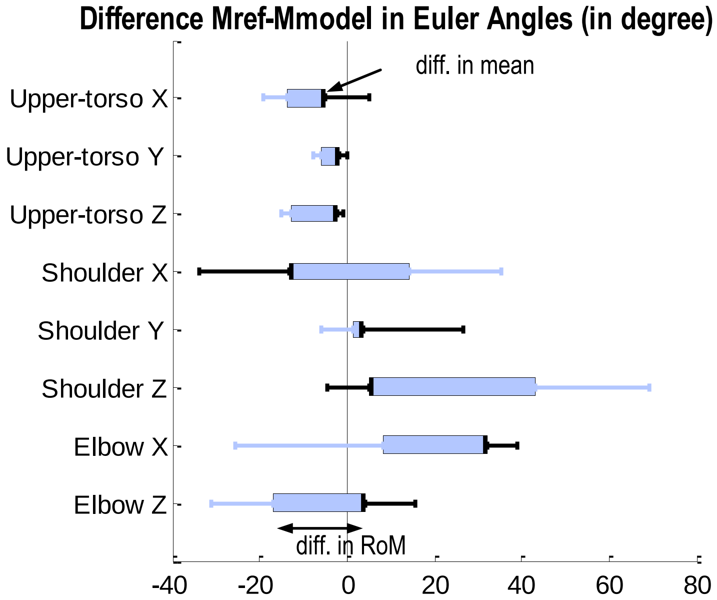

Figure 8: Difference of Euler angle mean and range of motion (RoM) between Mref and Mmodel. The black bars represent the differences in term of mean whereas the blue boxes represent the differences in term of range of motion.

The differences between Mref and Mmodel for the mean Euler angle and the range of motion obtained between the movements performed by the three subjects are presented on Figure 3 for each degree of freedom.

For the upper-torso angles, the differences in mean and in range of motion are low, which means that there is no important offset or important deviation in the measurements. The biomechanical model proposed is then satisfactory for the upper-torso.

For the X shoulder axis and the X elbow axis, differences of respectively 13° and 32° were noticed between the two measures for the mean whereas a difference of RoM from respectively 27 and 23° was noticed between the two sets of data. The offsets are probably due to calibration of the body axes during the N pose. The arms are probably not completely aligned with the vertical, which should be particularly true for the forearm due to the carrying angle existing between the longitudinal axes of the two segments. Since the axes obtained with the two biomechanical models are not aligned, the ranges of motion are also affected.

It should be checked that from one measure to the other with the same subject, these offsets remain the same in order to insure that one can compare the measure from the PAMAP system from one measurement session to the other.

The correlation (Table 1) between the angles Mmodel and the angles Mimu are reasonable taking into account the previous remarks. The limited correlation between the angles obtained through the two methods for the torso y angle and the elbow z angles can be explained by the reduced rotation around these axes.

According to these results, if the differences between the two methods are repeatable for one subject, one can conclude that the biomechanical model proposed within the PAMAP system is adequate. We should then therefore confirm this repeatability of the measures obtained by the PAMAP biomechanical model by realising additional experiments.

Table 1: Coefficient of correlation (r) between the Euler angles Mref and Mmodel.

r	Torso X	Torso Y	Torso Z	Shoulder X	Shoulder Y	Shoulder Z	Elbow X	Elbow Z
Subject 1	0.96	0.80	0.85	0.92	0.70	0.54	0.92	0.71
Subject 2	0.83	0.57	0.74	0.79	0.53	0.85	0.97	0.62
Subject 3	0.88	0.33	0.80	0.87	0.74	0.78	0.93	0.68
Mean	0.89	0.56	0.80	0.85	0.70	0.75	0.93	0.65
SD	0.07	0.23	0.06	0.06	0.09	0.15	0.04	0.12

1.2.3 *Validation of the measurement device: Mmodel vs Mimu*

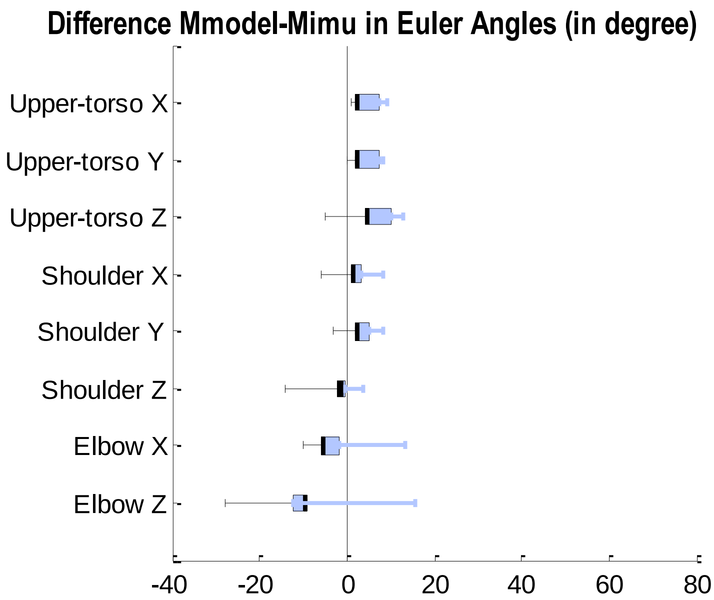

Figure 9: Difference of Euler angle mean and range of motion (RoM) between Mmodel and Mimu. The black bars represent the differences in term of mean whereas the blue boxes represent the differences in term of range of motion.

Taking into account that the reflective markers might not have been perfectly well aligned with the real axes of the IMUs, the agreement between the angles obtained with the reference motion capture system and the PAMAP body tracking system can be considered as being really good as illustrated by Figure 4. The difference between both means was indeed always below 10° for the mean differences and 5° for the RoM.

The correlation (Table 2) confirms the good consistency between the Euler angles obtained thanks to the validated optoelectronical motion capture system and thanks to the PAMAP system. As mentioned previously, the relatively poor coefficient of correlation obtained for the through the two methods for the torso y angle and the elbow z angles can be explained by the reduced rotation around these axes.

More data should complete this analysis. However, according to these preliminaries results, we can consider the PAMAP system as providing accurate data.

Table 2: Coefficient of correlation (r) between the Euler angles Mmodel and Mimu.

r	Torso X	Torso Y	Torso Z	Shoulder X	Shoulder Y	Shoulder Z	Elbow X	Elbow Z
Subject 1	0.92	0.82	0.84	0.73	0.78	0.78	0.90	0.70
Subject 2	0.91	0.77	0.89	0.88	0.74	0.85	0.96	0.62
Subject 3	0.88	0.00	0.80	0.87	0.74	0.78	0.93	0.68
Mean	0.90	0.53	0.84	0.84	0.78	0.77	0.92	0.67
SD	0.02	0.46	0.04	0.06	0.06	0.09	0.04	0.13

1.3 Performance of activity intensity estimation and activity classification

This part of the evaluation aims at evaluating the aerobic activity monitoring system of PAMAP. This activity monitoring system has two main goals. On the one hand, the system classifies miscellaneous activities performed during an individual's daily routine according to their intensity level – in respect of the recommendations for physical activity (Haskell et al. 2007) – as activities of light, moderate or vigorous effort. On the other hand, the system identifies the aerobic activities traditionally recommended with a high reliability. These recommended aerobic activities are walking, running, cycling and Nordic walking. In addition, the system also aims to identify the basic postures lying and sitting/standing, so that with the PAMAP system, most of an individual's daily routine can be described from the physical activity point of view.

1.3.1 Data collection

For the evaluation of the above mentioned goals of the PAMAP system, a large dataset – including the basic activities, but also others e.g. vacuum cleaning or playing soccer – has been recorded. The data collection is described within this section.

To obtain inertial data, 3 Colibri inertial measurement units (IMU) from Trivisio were used. For this part of the PAMAP system, only accelerometer data was used from the IMUs. The accelerometers have a resolution of 0.038 ms^{-2} in the range of ±16g. From the 3 IMUs, one was attached over the dominant wrist on the lower arm, one on the chest of the test subjects, and one sensor was foot-mounted. A Sony Vaio VGN-UX390N UMPC was used as inertial data collection unit, carried by the subjects in a pocket fixed on their belt. The placement of the sensors and this data collection unit is shown in Figure 10. The IMUs were attached to the data collection unit by USB-cables, which were taped to the body so that they did not restrict normal movements of the subjects.

Figure 10: Placement of IMUs and the data collection unit

During data collection, a supervisor accompanied the test subjects and marked the beginning and end of each of the different activities. This time stamped labels were also stored on the data collection unit. Synchronization of the time stamped acceleration data and annotations was done offline. Eight subjects (aged 27.88 ±2.17 years, BMI 23.68 ±4.13 kgm^{-2}, seven males and one female) were recruited among DFKI employees. Approximately 8 h of data were collected altogether.

The protocol for the data collection is described in Table 3 and Table 4. A criterion for selecting activities was on the one hand that the basic activities (walking, running, cycling and Nordic walking) and postures (lying, sitting and standing) to be recognized should be included. On the other hand, everyday (ascending and descending stairs), household (ironing, vacuuming) and fitness (playing soccer, rope jumping) activities were also included to cover a wide range of activities. A total of 14 different activities were included in the data collection protocol. The protocol was split into an indoor and an outdoor scenario, mainly because of the limited battery time of the collection unit, but also to avoid the overloading of the test subjects.

Table 3: Indoor protocol of data collection

Activity	Code	Intensity level [METs]	Duration [Min]
Lie	07011	1.0	3
Sit	09040	1.8	3
Stand	09050	1.8	3
Iron	05070	2.3	3
Break			1
Vacuum	05043	3.5	3
Break			1
Ascend stairs	17130	8.0	1
Break			2
Descend stairs	17070	3.0	1
Break			1
Ascend stairs	17130	8.0	1
Descend stairs	17070	3.0	1

Table 4: Outdoor protocol of data collection

Activity	Code	Intensity level [METs]	Duration [Min]
Walk very slow	17151	2.0	3
Break			1
Normal walk	17190/17200	3.3-3.8	3
Break			1
Nordic walk	—	4.0-6.0	3
Break			1
Run	12020/12030	7.0-8.0	3
Break			2
Cycle	01010	4.0	3
Break			1
Run	12020/12030	7.0-8.0	2
Normal walk	17190/17200	3.3-3.8	2
Break			2
Soccer	15610	7.0	3
Break			2
Rope jump	15551/15552	8.0-10.0	2

The ground truth for the activity recognition task is provided by the labels made during data collection. The first and last 15 seconds of data from each performed activity was discarded to avoid transient data. As for the intensity estimation task, since the aim of the system is to only estimate whether a performed activity is of light, moderate or vigorous effort, no precise measurements on an individual's oxigen consumption (e.g. with a portable cardiopulmonary system) is needed. Therefore, it is sufficient to use the Compendium of Physical Activities (Ainsworth et al. 2000) to obtain reference data for the intensity estimation task. This compendium contains MET levels assigned to 605 activities, and was also used in the recommendations (Haskell et al. 2007) to provide example activities of moderate and vigorous intensities. In the data collection protocol (cf. Table 3 and Table 4), the MET values from the compendium are also included together with the 5-digit activity codes used in the compendium. These MET levels can be used to distinguish activities of light intensity (< 3.0 METs), moderate intensity (3.0-6.0 METs) or vigorous intensity (> 6.0 METs), which provides the reference data required for the intensity estimation task: lying, sitting, standing, ironing and walking very slow are regarded as activities of light effort; vacuuming, descending stairs, normal walking, Nordic walking and cycling as activities of moderate effort; and ascending stairs, running, playing soccer and rope jumping as activities of vigorous effort.

1.3.2 Data processing

After the above described data collection and pre-processing steps, synchronized, time stamped and labeled acceleration data from the 3 IMUs is available. From the 3D-acceleration data, standard signal features were calculated over a window of 512 samples (about 5 s of data), in both time and frequency domain. Time-domain features were mean, median, standard deviation, peak acceleration and absolute integral. For the frequency-domain features, the DC component was first removed then the power spectral density (PSD) was calculated. Frequency-domain features were peak frequency of the PSD, power ratio of the frequency bands 0-2.75 Hz and 0-5 Hz, energy of the frequency band 0-10 Hz and spectral entropy of the normalized PSD on the frequency band 0-10 Hz. The signal features extracted from the 3D-acceleration data are computed for each axis separately and then for the 3 axes together. Moreover, since synchronized data from the 3 IMUs is available, combining sensors of different placements is possible. From the above mentioned features mean, standard deviation, absolute integral and energy calculated on 3 axes of each of the IMUs are pair wise (e.g. hand + chest sensor placement) weighted accumulated, and a weighted sum for all the 3 sensors together is also added.

For the intensity estimation task, the goal is to distinguish activities of light, moderate and vigorous effort. For the first prototype of the PAMAP system, a very simple approach was selected by using the best feature with appropriate thresholds for solving this classification problem. To identify the feature having the best performance in discriminating these intensity classes, the measure presented in [Huynh et al. 2005] was applied. The K-means algorithm with k = 100 clusters was used for clustering different features. The fraction for each cluster and intensity class was then computed, and the cluster precisions for each intensity class were obtained from the fractions.

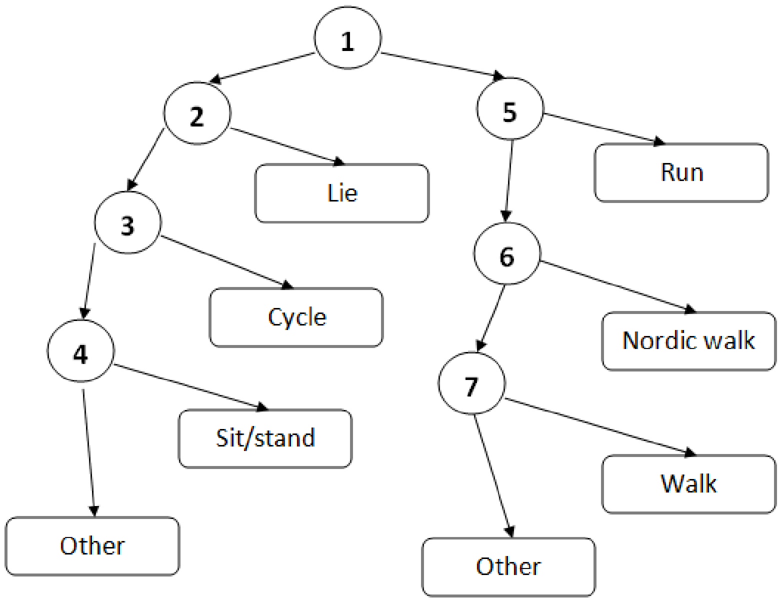

Figure 11: Placement of IMUs and the data collection unit

For the activity classification task, a custom decision tree was selected in the first prototype, the structure of the tree is depicted in Figure 11. The tree has 7 binary decision nodes and 8 leaf nodes, the latter representing the activities. The first decision node divides all activities into activities with and without footsteps, all other decisions are used to separate one activity from the remaining other activities. If the current sample is not recognized into any of the activities while passing the decision tree, it falls through to the default "other" class. The signal features used in the decision nodes are the following (the numbers in the list correspond to the numbers in the decision nodes):

1. absolute integral of the accelerations summarized for the 3 axes measured on the foot-mounted sensor
2. peak absolute value of the up-down (transversal) acceleration measured on the chest sensor
3. energy of the accelerations summarized for the 3 axes measured on the foot-mounted sensor
4. standard deviation of the up-down (transversal on initial position) acceleration measured on the lower arm sensor

5. median value of the forward-backward (horizontal) acceleration measured on the foot-mounted sensor
6. peak absolute value of the forward-backward (coronal on initial position) acceleration measured on the lower arm sensor
7. peak frequency value of the up-down acceleration measured on the foot-mounted sensor

1.3.3 *Validation of activity intensity estimation*

For the intensity estimation task, the following feature was identified as the feature having the best performance to classify samples into the intensity classes: standard deviation of the up-down (transversal) acceleration measured on the chest sensor. Figure 7 shows the confusion matrix for this feature, the overall performance is 87.54%. It is worth to note, that misclassifications only appear into "neighbour" intensity classes, thus no samples annotated as light intensity were classified into the vigorous intensity class, and vice versa.

Annotated intensity	Estimated intensity 1	Estimated intensity 2	Estimated intensity 3	Performance [%]
1	10414	1838	0	85.00
2	319	10924	44	96.78
3	0	1512	4751	75.86

Figure 12: Confusion matrix of the intensity estimation task for the feature: standard deviation of the up-down acceleration on the chest sensor

More information can be obtained from Figure 8, which shows how samples of different activities were classified into the intensity classes. For instance it shows that the selected feature performed very well on estimating the intensity of samples belonging to postures (lying, sitting and standing). Good to very good results were achieved on samples of household activities (ironing and vacuuming), and of sport activities (running, cycling, playing soccer and rope jumping). In contrast, performance was poor on samples of the activities walking very slow and ascending stairs. The reason is that the characteristic of these activities overlap with normal walking from the selected feature's point of view. Moreover, due to the similarity of the movement, it is reasonable to expect that the samples of ascending stairs cannot be distinguished from walking related activities of moderate effort with only features derived from acceleration data, which implies the need for features extracted from physiological measurements, e.g. heart rate data.

Annotated activity	Estimated intensity 1	2	3	Performance [%]
Lie	2329	33	0	98.60
Sit	2259	0	0	100.00
Stand	2429	110	0	95.67
Iron	3093	128	0	96.03
Vacuum	196	2393	0	92.43
Ascend stairs	0	1319	12	0.90
Descend stairs	0	865	25	97.19
Walk very slow	304	1567	0	16.25
Normal walk	0	3462	19	99.45
Nordic walk	0	2055	0	100.00
Run	0	0	2913	100.00
Cycle	123	2149	0	94.59
Soccer	0	178	1078	85.83
Rope jump	0	15	748	98.03

Figure 13: Detailed confusion matrix of the intensity estimation task for the feature: standard deviation of the up-down acceleration on the chest sensor

Two other features, extracted from acceleration data, performed — for both the overall performance as for the detailed results on the different activities — similarly, as the above presented feature: the peak absolute value summarized for the 3 axes measured on the chest sensor, and the weighted sum of the standard deviation for all the 3 sensors together. The latter underlines, that if synchronized data from different sensor placements is available, it is worth to extract and investigate features calculated from multiple sensors for the intensity estimation task.

It is planned to incorporate features extracted from heart rate data in addition to the features extracted from acceleration data used in the results presented above. It is expected, that by combining acceleration and heart rate related features, the performance of the system on the intensity estimation task can be improved.

1.3.4 Validation of activity classification

For the activity classification task, the goal was to recognize basic aerobic activities and postures from a larger set of activities, and classify all other activities into the default "other" class. The results of the classification are shown in the confusion matrix of Figure 9, the overall performance is 86.80%. The results demonstrate, that the classifier works very good-good on the basic recommended activities (like normal walking or cycling), and also performs well on other activities (like ironing or rope jumping). Most of the misclassifications can be explained from the data collection and the characteristic of certain activities, e.g. the overlapping of the characteristic of ironing with standing, or the similarity between running with the ball during playing soccer and just running.

Annotated activity	Estimated activity Lie	Sit/ Stand	Normal walk	Nordic walk	Run	Cycle	Other	Performance [%]
Lie	2341	12	0	0	0	4	0	99.32
Sit	0	2035	0	0	0	0	155	92.92
Stand	0	1754	0	0	0	11	729	70.33
Normal walk	0	0	2916	0	0	0	32	98.91
Nordic walk	0	0	242	983	5	0	419	59.61
Run	0	0	0	37	2275	0	23	97.43
Cycle	0	0	0	0	0	1351	513	72.48
Iron	0	350	0	0	0	0	2956	89.41
Vacuum	3	0	0	0	0	150	2150	93.36
Ascend stairs	0	0	18	0	0	59	1300	94.41
Descend stairs	0	0	23	0	0	66	807	90.07
Soccer	0	0	78	145	227	0	801	64.03
Rope jump	0	0	40	39	4	11	660	87.53

Figure 14: Confusion matrix of the activity classification task

1.4 Sensor fastening

Two different ways of fastening the sensors have been proposed (deliverable D4.2). These two systems are illustrated on Figure 10. The first one that includes bandages is quite similar to that used by different companies. Therefore, their advantages and drawbacks are already known. The second method includes a "second-skin" suit and Velcro fasteners. This method had to be tested in order to check whether the relative high inertia of the sensors provoked oscillation of the sensors that might disturb the measures.

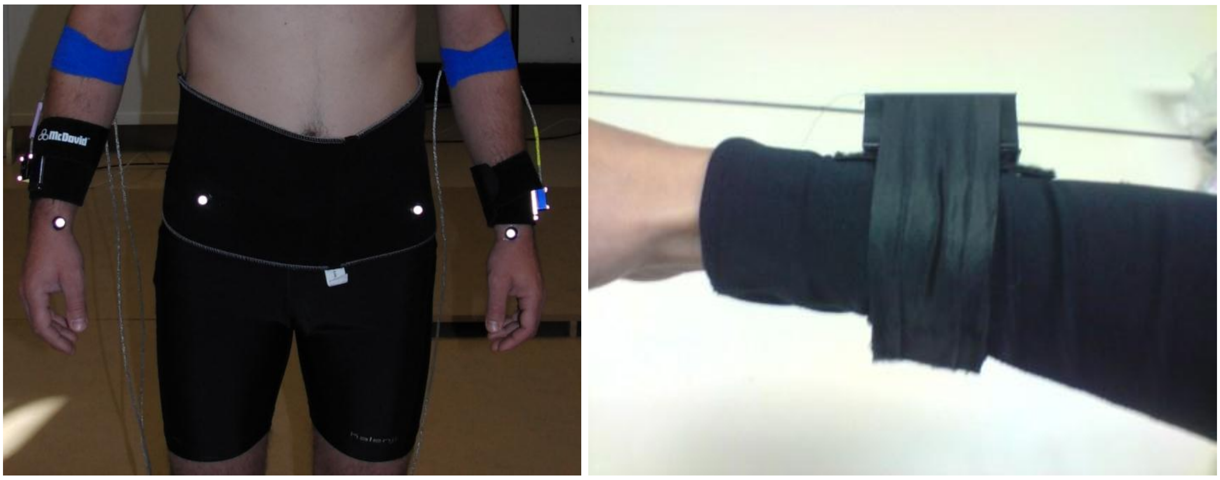

Figure 15: Sensor fastening based on bandages (on the left) and on a body suit and velcros (on the right).

1.4.1 Methodology

The last prototype of the IMUs was not available to perform these tests. Therefore, alterantive sensors having the same inertia and size as the real sensors were created.

The real sensors have a dimension of 56*42*19mm for a weight of 48g, which makes a density of 1.0741g/cm^3. PVC that has a density of 1.190 g/cm^3 was then chosen to create these alternative sensors.

An optoelectronical motion capture system (Vicon, Oxford Metrics) was used to measure the trajectories of reflective markers placed on the IMUs but also of reflective markers placed at immediate proximity of the IMUs directly on the suit worn by a subject.

The subject performed different movements that imply high accelerations such as jumping and moving his arms fast.

The reflective markers weighting less than 3g, the comparison of the acceleration of the markers placed on the IMUS and on those placed on the body suit enables the estimation of the effect of sensor inertia on the measurements.

To perform the evaluation of IMU inertia effects on measures, the acceleration of sensors and its time-domain frequency analysis of the markers were compared.

1.4.2 Validation

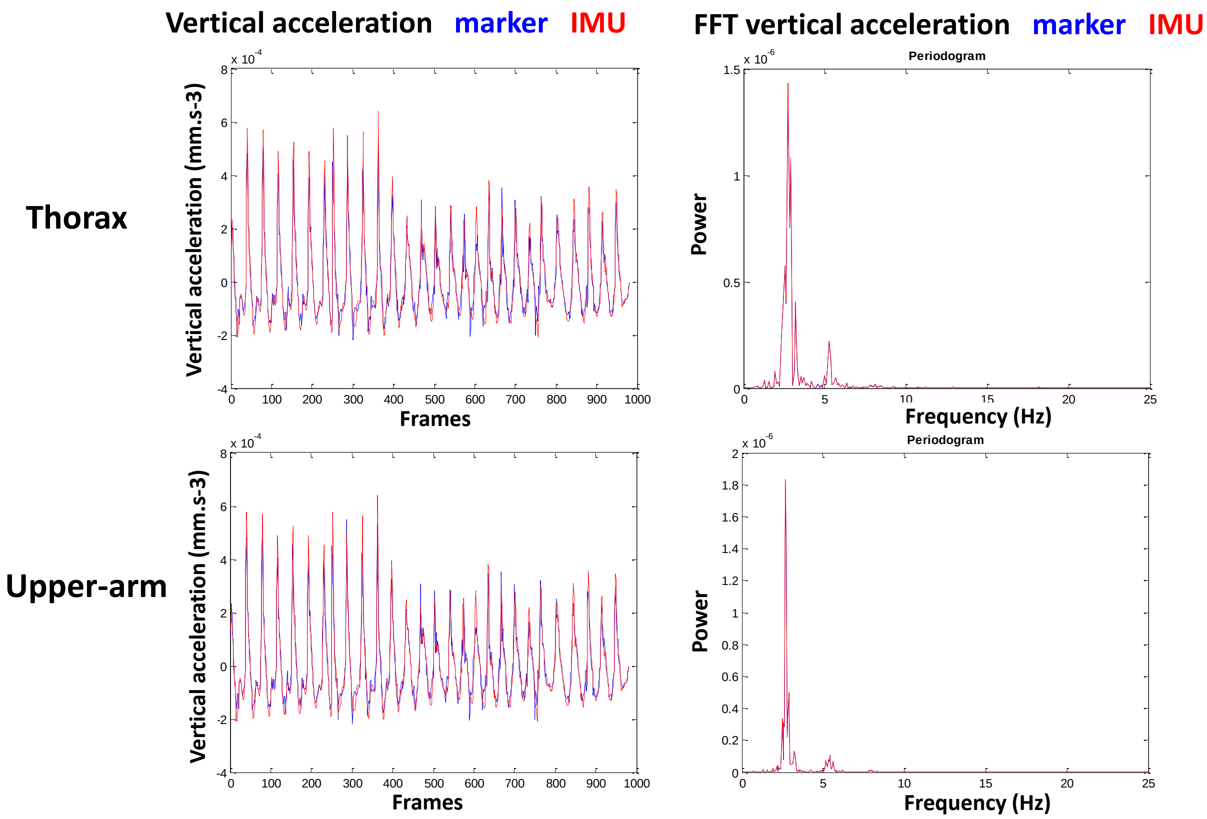

Figure 16: Acceleration (on the left) and time-frequency analysis (on the right) of markers placed on the thorax (on the top) and on the upper-arm (on the bottom).

During the movements, no notable differences were noticed between the acceleration of the markers placed on the IMUs and those placed directly on the body suit. This was true whatever the movement performed and the markers position. Figure 11 illustrates this for the markers placed on the thorax and on the upper-arm. As it can be seen, no difference in term of amplitude or frequency was measured between the acceleration of the markers placed whether directly on the body suit, whether on the IMUs.

Therefore, it can be conclude that the use of a bodysuit combined with Velcro-fastener is suitable for an accurate body tracking with the PAMAP system.

Besides the information acquisition system (the hardware platform and associated information extraction technology) that has been evaluated in the previous sections, another major component of the PAMAP system is the information management system, consisting of the infrastructure and a set of applications that facilitate out-of-hospital physical activity monitoring for both prevention and rehabilitation. This is described in D5.2 (First PAMAP System Software). A part of the information management system consists in an Electronic Health Record, which takes the form of a web application for collecting and managing a comprehensive summary of the medical record of the monitored subjects, a rehabilitation plan management module and a health status surveys module.This first software test was done in the period between October and December 2010 and included regular contacts between ICOM and CIT-INSERM. The rationale of this testing was twofold: first, to identify dysfunctions of the first software prototype; and second, to identify possible functional enhancements of this prototype. Some clinical case data have been recorded using the EHR for that purpose. These data included anthropometric values, familial and personal history, diagnostics, therapies, and results of functional tests. This first approach allowed detecting some minor dysfunctions and several issues.

Among the issues that were discussed between ICOM and CIT-INSERIM and taken into consideration by the former partner towards the release of a new version where the following:

- A request by CIT-INSERIM to modify the EHR interface so as to better fit to the physicians' available time for editing a new patient record was expressed
- In the Diagnosis Management tab of the intLIFE EHR it was requested to add a new set of diagnosis lists to pick up from, based on a specialty categorization (this is provided as Annex).
- The information included in the Care Plan tab of the intLIFE EHR has undergone a major restructure. Reports and Today Schedule sub-tabs have been added. The former provides to the clinician an overview of the answers that have been provided by the patient in questionnaires or manually inserted vital signs measurements, while the latter provides to the patient the possibility to review via the web interface –instead of the i-TV interface- the activities that are scheduled for the current day.
- The Body Mass Index sub-tab has been removed from the Visits tab and added to the Health Profile tab.
- The tests list under the Tests tab have been enhanced with several Functional Capacity and Activity Monitoring Tests. After a literature review of the modalities of mental and physical assessment in aging people and cardiac patients, a big quantity of tests and scales required for patients' functional and mental assessment have been identified. Patients' assessments validated methods are indeed very numerous and their choice partly depends on what the physician wishes to improve using the rehabilitation program. The tests, questionnaires and scales mostly used were selected and made available in the software.
- For the Six Minutes Walking Tests an automatic calculation of the normal values for the covered distance was added in order for the clinicians to compare it to the actual distance covered by the subject. The software implements 2 equations (Troosters et al., 1999, and Enright and Sherill, 1998).
    - Troosters et al., 1999 : Distance = 218 + (5.14 x height) – (5.32 x age) – (1.80 x weight) + (51.51 x sex), with distance in meters, height in centimeters, age in years, weight in kilograms, sex 1 for men and 0 for women.

- Enright and Sherill, 1998 : For men : Distance = (7.57 x height) – (5.02 x age) – (1.76 x weight) – 309, For women : distance = (2.11 x height) – (5.78 x age) – (2.29 x weight) + 667, with distance in meters, height in centimeters, age in years and weight in kilograms.

As a conclusion, it can be said that after the first assay that the EHR seems easy to use; it can be very accurate related to the quantity and accuracy of data that can be recorded. However, it is so complete that more time is necessary to better assess it through all its tabs and dropdown menus. This will be done regularly all along the PAMAP project duration until the clinical assay.

3 CONCLUSION

The technical evaluation of the system components shows that this first version of the hardware platform and associated information extraction technology are suitable to enable physical activity monitoring. The information management system evaluation is also suitable since it has been evaluated as being satisfactory by the end-user.

This first evaluation mainly consisted in a functional evaluation on a component level to ensure the functionality of the individual system components. The system will be evaluated altogether within the second evaluation phase, which will be earlier than originally planned in order to have some time for final improvements before the end of the project.

Specialities[1]

Cardiology
Dermatology
Endocrinology
Hematology
Hepato-Gastroenterology
Immunology
Infectious diseases
Neurology
Ophtalmology
Orthopedics
Pulmonology
Rheumatology
Urology-Nephrology

Main Diagnostics per Speciality

CARDIOLOGY

Abdominal aortic aneurysm
Acute lower limb ischemia
Acute pericarditis
Aortic Dissection
Aortic insufficiency
Aortic stenosis
Arrhythmia
Atrioventricular block
Bruit, vascular murmur
Cardiogenic shock
Chest pain
Congenital cardiopathy
Coronary disease
Coronary heart disease (CHD)
Cyanosis
Deep vein thrombosis of lower limbs
Dilated cardiomyopathy
Dyspnea
Edema
Essential hypertension
Genetic heart disease
Heart murmur
Hypertrophic cardiomyopathy (HCM)
Implantable defibrillator
Infective endocarditis
Ischemic cardiomyopathy
Left ventricular failure
Lower limb arterial occlusive disease
Malignant hypertension / hypertensive emergencies
Mitral regurgitation

[1] (http://www.medinfos.com/principales/urologie.shtml)

Mitral stenosis
Muscle fatigue
Myocardial infarction
Pacemaker
Palpitations
Pulmonary embolism
Right heart failure
Secondary hypertension
Tamponade and constrictive pericarditis
Unconsciousness
Valve prostheses
Vascular murmur, bruit

ENDOCRINOLOGY

Acromegaly
Acute metabolic complications of diabetes
Adrenal insufficiency or Addison's disease
Diabetes mellitus
Dyslipidemia
Goiter or thyroid nodule
Hypercortisolism
Hyperprolactinemia
Hyperthyroidism
Hypoglycemia
Hypopituitarism
Hypothyroidism
Non-insulin dependent diabetes
Pheochromocytoma
Polyuropolydipsic syndrome
Primary hyperparathyroidism
Thyroid cancer
Thyroiditis

HEMATOLOGY

Acute lymphoblastic leukemia
Acute myeloid leukemia
Adenopathy
Anemia: pathophysiology, classification, diagnosis and treatment
Autoimmune hemolytic anemia
Bone marrow failure
Chronic lymphocytic leukemia
Chronic myeloid leukemia
Defibrination syndrome
Disseminated intravascular coagulation (DIC) and fibrinolysis
Haemorrhagic syndrome
Hemophilia and von Willebrand disease
Hodgkin's disease
Idiopathic thrombocytopenic purpura
Inflammatory anemia
Iron deficiency anemia
Macrocytic anemia
Malignant non-Hodgkin lymphoma
Mononucleosis

Multiple myeloma or Kahler's disease
Myelofibrosis
Plasma cell dyscrasia
Polycythemia vera or Vasquez disease
Purpura
Refractory anemia
Sickle Cell Disease
Splenomegaly
Thalassemias
Thrombocytopenia
Waldenström's disease or Waldenström macroglobulinemia

HEPATO-GASTROENTEROLOGY

Acute diarrhea
Acute pancreatitis
Alcoholic cirrhosis
Ascites
Cholelithiasis
Chronic diarrhea
Chronic pancreatitis
Colorectal cancer
Complications of gallstones
Constipation
Crohn's disease
Endocrine pancreatic tumors
Epigastric pain
Esophageal cancer
Gastrointestinal bleeding
Helicobacter pylori and peptic ulcer disease
Hemochromatosis
Hepatomegaly
Hepatopathy and non-alcoholic cirrhosis
Hiatal hernia and gastroesophageal reflux
Hypergastrinemia
Inflammatory bowel disease
Jaundice with conjugated bilirubin
Malabsorption syndromes
Non-cirrhotic alcoholic hepatopathy
Pancreatic cancer
Pathology of stomach surgery
Peptic ulcer (PU) or gastroduodenal ulcer
Portal hypertension
Primary liver cancer
Stomach cancer
Ulcerative colitis
Viral Hepatitis

IMMUNOLOGY

Amyloidosis
Gougerot-Sjögren syndrome
Lupus erythematosus
Polyarteritis nodosa
Polymyositis and dermatomyositis

Raynaud's phenomenon and scleroderma
Vasculitis

INFECTIOUS DISEASES

AIDS and HIV infection
Arboviruses
Aseptic meningitis
Brucellosis
Eosinophilia
Erythema nodosum
Fever after returning from a tropical country
Flu
Gram negative infection and septic shock
Hepatic amoebiasis
Hepatic echinococcosis
Influenza A (H1N1)
Influenza A (H5N1) or H5N1 avian influenza
Intestinal amebiasis
Leprosy
Leptospirosis
Malaria
Pneumococcal disease
Prolonged fever
Purulent meningitis
Rickettsial infection
Schistosomiasis
Sepsis syndrome
Staphylococcal infections or staph infections
Streptococcal infections
Syphilis
Trypanosomiasis
Typhoid or typhoid fever
Visceral leishmaniasis or Kala-Azar

NEUROLOGY

Amyotrophic Lateral Sclerosis
Cauda equina syndrome (CES)
Cerebellar syndrome
Coma
Dizziness
Epilepsy
Hemiplegia
Intracerebral hematoma
Intracranial hypertension
Multiple Sclerosis
Myasthenia
Non-traumatic subarachnoid hemorrhage
Parkinsonian syndromes
Polyneuritis and mononeuropathies
Polyradiculoneuritis and Guillain-Barre
Spinal cord compression
Stroke
Syringomyelia

Transient ischemic attacks
Trouble walking and balance disorder

PULMONOLOGY

Asthma
Severe acute asthma
Obstructive syndrome
Restrictive syndrome
Chronic Obstructive Pulmonary Disease
Sleep apnea-hypopnea syndrome (SAHS)
Broncho-pulmonary primary
Bronchiectasis
Dyspnea
Effusion of the pleura
Hemoptysis
Chronic obstructive respiratory insufficiency
Sarcoidosis
Purulent pleurisy or empyema
Lung abscesses
Acute infectious pneumonia
Mediastinal compression syndrome
Pneumothorax
Pulmonary tuberculosis and primary tuberculous infection

RHEUMATOLOGY

Algodystrophies
Ankylosing spondylitis
Bacterial discitis
Chondrocalcinosis
Coxarthrosis
Fatigue
Fiessinger-Leroy-Reiter Syndrome (oculo-urethral-synovial syndrome)
Gout and hyperuricemia
Hypercalcemia
Juvenile chronic arthritis (JCA)
Lumbago and sciatica
Osteoporosis and osteomalacia
Paget's Disease
Polymyalgia rheumatica (or rhizomelic pseudopolyarthritis) and Horton disease (or temporal arteritis)
Post-streptococcal arthritis
Psoriatic arthritis
Rheumatoid arthritis
Rheumatoid arthritis (acute and chronic)
Spondyloarthropathies and reactive arthritis
Stress fractures

ORTHOPEDICS

Fractures
Highway accident
Joint pain
Ligament injuries
Tendon injuries

UROLOGY-NEPHROLOGY

Acute nephritic syndrome
Acute renal failure
Chronic renal failure
Dehydration
Disorders of acid-base balance
Hematuria
Henoch-Schoenlein purpura (HSP) or rheumatoid purpura
Hyperhydration
Hyperkalemia and hypokalemia
Hyponatremia and hypernatremia
Nephrolithiasis
Nephrotic syndrome
Polycystic kidney
Proteinuria
Urogenital tuberculosis

DERMATOLOGY

Acanthosis nigricans
Achromie
Acné
Acné rosacée ou rosacée
Alopécie
Amyloïdose
Angiodermite
Angiome stellaire
Anthrax staphylococcique
Aphtose
Atrophie
Balanite
Behçet (maladie de)
Bowen (maladie de)
Candidose
Carcinome basocellulaire
Carcinome spinocellulaire
Chancre mou
Couperose
Darier (maladie de)
Degos (maladie de)
Dermatite actinique chronique
Dermatite atopique
Dermatite herpétiforme
Dermatophytose
Dermite péri-orale
Dermite séborrhéique
Dermographisme
Dyshidrose
Eczéma
Épidermolyse bulleuse
Érythème noueux
Érythème pigmenté fixe
Érythème polymorphe

Erythrasma
Érythrodermie
Escarre
Fiessinger-Leroy-Reiter (syndrome de)
Folliculite
Furoncle
Gale
Gangrène
Granulome annulaire
Herpès
Ichtyose
Impétigo
Intertrigo
Kératose actinique
Kératose pilaire
Leishmaniose
Lèpre
Leucokératose
Lichen plan
Lichen scléro-atrophique
Livedo
Lupus érythémateux
Mal perforant plantaire
Maladie professionnelle
Mastocytose
Mélanome
Miliaire
Molluscum contagiosum
Mucinose
Myases
Nécrobiose lipoïdique
Œdème de Quincke
Panniculite
Papillonite
Parakératose achromiante
Parapsoriasis en gouttes
Pédiculose
Pelade
Pemphigoïde bulleuse
Pemphigus
Péri-onyxis
Perlèche
Photodermatose
Pityriasis rosé de Gibert
Pityriasis versicolor
Poïkilodermie
Porphyries
Prurigo
Psoriasis
Purpura
Rosacée ou acnée rosacée
Sarcoïdose
Scarlatine

Sycosis
Syndrome bouche-main-pied
Syndrome de Lyell
Syndrome de Stevens-Johnson
Syphilis
Teigne
Toxidermie bulleuse
Trombidiose
Tuberculose
Tungose
Urticaire
Varicelle
Vascularite nécrosante
Verrue
Vitiligo
Vulvo-vaginite
Xanthome
Xeroderma pigmentosum
Zona

OPHTALMOLOGY

Anomalies pupillaires
Cataracte
Choroïdite ou uvéite postérieure
Conjonctivites infectieuses
Conjonctivites non infectieuses
Corps flottants ou myodésopsies
Décollement de rétine
Dégénérescence maculaire
Distrophies et dégénérescences cornéennes
Dystrophies rétiniennes
Episclérite et sclérite
Glaucome
Inflammation cornéenne
Iridocyclite
Nystagmus
Occlusion veineuse rétinienne
Œdème papillaires et atrophie optique
Pathologie orbitaires
Paupières : anomalies de position
Paupières : blépharites, dermatites et tuméfactions
Rétinopathie diabétique
Rétinopathie pigmentaire ou iritis
Sécrétion lacrymale et drainage
Strabisme
Traumatisme du globe oculaire
Traumatisme : paupières, orbite, crâne
Tumeurs intraoculaires
Uvéite antérieure